

1 **Upstream Urbanization Exacerbates Urban Heat Island Effects**

2 Da-Lin Zhang¹, Yi-Xuan Shou^{1,2} and Russell R. Dickerson¹

3 ¹Department of Atmospheric and Oceanic Science
4 University of Maryland, College Park, Maryland 20742

5 ²National Satellite Meteorological Center, China Meteorological Administration, Beijing,
6 P. R. China

7
8
9
10
11 *Geophysical Research Letter*

12 Submitted: September 2009

13 Revised: November 2009

14
15
16
17
18
19 Corresponding author:
20 Dr. Da-Lin Zhang
21 Department of Atmospheric and Oceanic Science
22 University of Maryland
23 College Park, Maryland 20742-2425
24 Tel. (301) 405-2018
25 Fax: (301) 314-9482
26 Email: dalin@atmos.umd.edu
27

28
29
30
31
32
33
34
35
36
37
38
39
40
41
42

Abstract

Urban Heat Island (UHI) effects adversely impact weather, air quality, and climate. Previous studies have attributed UHI effects to localized, surface processes. Based on an observational and modeling study of an extreme UHI (heat wave) episode in the Baltimore metropolitan region, we find that upstream urbanization exacerbates UHI effects and that meteorological consequences of extra-urban development can cascade well downwind. Under southwesterly wind, Baltimore, MD, experienced higher peak surface temperatures and higher pollution concentrations than did the larger urban area of Washington, DC. Ultra-high resolution numerical simulations with National Land Cover Data (NLCD) of 2001 show a nonlocal, dynamical contribution to UHI effects; when the upstream urban area is replaced by natural vegetation (in the model) the UHI effects could be reduced by more than 25%. These findings suggest that judicious land-use and urban planning, especially in rapidly developing countries, could help alleviate UHI consequences including heat stress and smog.

43 **1. Introduction**

44 There is considerable evidence that changes in land use, especially urbanization, can
45 change local climate (e.g., Oke 1987; Bornstein and Lin 2000; Kalnay and Cai 2003;
46 Rotach et al. 2005; IPCC 2007; Grossman-Clarke et al. 2008). Artificial surfaces increase
47 runoff, inhibit evapotranspiration, and increase absorption of solar radiation, in addition
48 to the heat directly emitted by fuel combustion and air conditioning. These urban heat
49 island (UHI) effects lead to heat stress in the summer and increased concentrations of the
50 air pollutants ozone (e.g., Banta et al. 1998; Cheng and Byun 2008; Jacob and Winner
51 2009; Bloomer et al. 2009) and fine particulate matter (PM_{2.5}) or haze (see
52 Supplementary Fig. A). The heat wave of 2003 is blamed for hundreds of excess deaths
53 in England and thousands in other European countries (e.g., Fischer et al. 2004; Stedman
54 2004). Herein we show that some heat wave events may be exacerbated by a nonlocal
55 dynamical impact that cascades from upwind urbanization. This will be achieved by
56 numerically simulating the extreme UHI (heat wave) episode of 7-10 July 2007 in the
57 Mid-Atlantic region of the eastern United States. This UHI episode exhibited a peak (2-
58 m) surface temperature (T_{sfc}) of 37.5°C with a maximum 8-h average ozone concentration
59 of 125 ppb and a maximum 24-h average particulate matter concentration of 40 $\mu\text{g m}^{-3}$ in
60 Baltimore (the current standards are 75 ppb and 35 $\mu\text{g m}^{-3}$), but concentrations were 85
61 ppb and 29 $\mu\text{g m}^{-3}$ in Washington where the peak T_{sfc} was 36.5°C. The contrast in UHI
62 intensity with respect to the similar rural surroundings and synoptic conditions can not be
63 explained by the city size and population (Oke 1973), since the Baltimore metropolitan
64 has a smaller urban area (and population) than that of Washington (see Fig. 1).

65 **2. Model description**

66 In this study, we used a multi-nested version of the Weather Research and Forecast
67 (WRF) model (Skamarock et al. 2005) coupled with a sophisticated single-layer urban
68 canopy model (UCM) (Kusaka et al. 2001; Chen and Dudhia 2001) at grid size as fine as
69 500 m. The quadruply nested domains of the coupled WRF-UCM model (Chen and
70 Dudhia 2001; Kusaka et al. 2001; Skamarock et al. 2005) have (x, y) dimensions of 181 ×
71 151, 244 × 196, 280 × 247, and 349 × 349 with the grid length of 13.5, 4.5, 1.5, and 0.5
72 km, respectively. The innermost domain covers an area that is about 60% greater than
73 that shown in Fig. 1. All the domains use 30 layers in the vertical with 20 layers in the
74 lowest 2 km in order to better resolve the evolution of the UBL.

75 The model is initialized at 1200 UTC (or 0700 LST) 7 July 2007 and integrated for
76 72 h until 1200 UTC 10 July 2007. The model initial conditions and its outermost lateral
77 boundary conditions as well as the soil moisture field are taken from the National Centers
78 for Environmental Prediction's (NCEP) 1° resolution Final Global Analyses.

79 The model physics schemes used include: (i) a three-class microphysical
80 parameterization (Hong et al. 2004); (ii) a boundary-layer parameterization (Janjić 1994);
81 (iii) a land-surface parameterization in which four soil layers and one canopy with 24
82 land-use categories are incorporated (Chen and Dudhia 2001); and (iv) an ensemble
83 cumulus scheme (Grell and Devenyi 2002) as an additional procedure to treat convective
84 instability for the first two coarsest-resolution domains.

85 The UCM (Kusaka et al. 2001) includes 3-category 30-m resolution urban surfaces
86 (i.e., low-intensity residential, high-intensity residential, and
87 commercial/industrial/transportation), based on the U.S. Environmental Protection
88 Agency's NLCD of Year 2001 - the most recent year for which high-resolution land-

89 cover data are available. The dynamic and thermodynamic properties of roofs, walls and
90 roads as well as some anthropogenic effects are used to specify roughness length, albedo,
91 emissivity and the other surface parameters influencing the surface energy budget.

92 **3. Results**

93 During this study period, the circulation was dominated by weak, westerly flows
94 until the late morning hours of July 9 when the surface winds backed to the southwest
95 (see Fig. 2b, and Supplementary Fig. B1). These are the two typical summertime flow
96 regimes under the influence of the Bermuda high. In the next, we will first verify the
97 model-simulated surface features before using the model results to examine the impact of
98 upstream urbanization on the extreme UHI and associated urban boundary layer (UBL).

99 *a. The UHI effects*

100 Skin temperature (T_{skin} , a radiometric temperature derived from the thermal
101 emission of the earth surface as some temperature average between various canopy and
102 soil surfaces) observed by the MODIS satellite instrument at 1745 UTC (1245 LST) 9
103 July 2007 shows pronounced contrasts between urban and rural areas (see Fig. 2a), in
104 agreement with contrasting land-cover categories (see Fig. 1). Minor differences in T_{skin} ,
105 e.g., over Columbia and Frederick, are likely due to rapid urbanization since 2001. The
106 satellite observations highlight UHI effects over Washington, Columbia, Baltimore,
107 Reston, and Frederick as well as many small towns. The hottest T_{skin} ($> 46^{\circ}\text{C}$) occurred
108 at the heart of these cities in areas of high intensity residential buildings and
109 commercial/industrial activity; they were more than 10°C higher than rural regions even
110 at this early afternoon hour.

111 The coupled model reproduces well the observed UHI intensities, especially the

112 sharp contrasts between urban, suburban and rural areas (see Figs. 2a,b), despite the use
113 of large-scale initial conditions. The model even captures the UHI effects of Interstate
114 highways such as I-70 between Frederick and Baltimore, and I-270 between Frederick
115 and Washington. In contrast, I-295, the Baltimore-Washington Parkway running
116 northeast-southwest between these two cities has tree cover in the median and off the
117 shoulders - it does not have a heat signature. The simulated UHI patterns resemble those
118 of the land-cover map even better than the satellite observations (see Figs. 1 and 2b),
119 because of the specified Year-2001 land-cover (NLCD) data in the model. The model
120 slightly overestimates the area of maximum T_{skin} and misses the UHI effects over some
121 towns, but this could again be attributed to land-use changes since 2001.

122 The urban area T_{sfc} at 2-m altitude, like T_{skin} , exhibits substantially more warming ($>$
123 5°C) than that over the rural area in the mid-afternoon (i.e., 1530 LST), and the
124 commercial-industrial-transportation areas, often located near a city's center, are $3\text{-}4^{\circ}\text{C}$
125 warmer than the suburbs (see Fig. 3a and Supplementary Fig. B1). The simulated peak
126 T_{sfc} at Baltimore and Washington are 36.5 and 35.5°C , respectively, as compared to the
127 observed 37.5 and 36.5°C . This 1°C negative bias is not detrimental to the present study,
128 since T_{sfc} is a diagnostic variable between T_{skin} and the model surface layer (centered at z
129 $= 12$ m) temperatures, but the 1°C T_{sfc} difference between Baltimore and Washington is
130 significant.

131 Figure 2b also shows general agreement between the simulated surface winds and
132 the few observations available. We see the convergence of southwesterly flows with the
133 Chesapeake Bay breeze, with urban surface winds $2\text{-}3\text{ m s}^{-1}$ weaker than those over rural
134 areas due to the presence of high roughness elements. Confluence of the two air streams

135 in the northeast portion of Baltimore led to an area of stagnant winds (Figs. 2b and 3a)
136 and locally high pollution (e.g., ozone) concentrations in the late afternoon of 9 July (see
137 <http://www.airnow.gov/>). The southwesterly flows began to intrude the study area near
138 noon 9 July, progressed onto Columbia by 1245 LST (see Fig. 2b), and passed over
139 Baltimore 3 h later (see Fig.3a).

140 *b. The upstream effects*

141 To reveal how the upstream urbanization (i.e., in Columbia and Washington) could
142 exacerbate the UHI effects over Baltimore, the southwesterly flows are superimposed on
143 the urban distribution of the Washington-Baltimore corridor. Figure 4a shows an along-
144 wind vertical cross section of in-plane flow vectors and the perturbation potential
145 temperature¹ θ' , through Columbia and Baltimore in the mid-afternoon of July 9, where
146 θ' is obtained by subtracting the mean potential temperature profile in the rural
147 environment to the west of Baltimore. The upward extension of the UHI effects with
148 different intensity layers extend up to ~ 1.4 km altitude, the approximate depth of the
149 well-mixed UBL at this time. The stratified UBLs appear as layered “hot plumes”
150 (columns of rising air) corresponding to individual local towns along the Washington-
151 Baltimore corridor (see Figs. 4a and 1). To our knowledge, previous studies have
152 examined the local UHI effects mostly in the context of T_{sfc} and T_{skin} , but with little
153 attention to such vertical UHI structures due to the lack of high-resolution data.
154 Moreover, deep rising motions on the scale of 10 – 20 km and as strong as 0.6 m s^{-1} occur
155 in the well-mixed UBL. These are unlikely due to gravity waves associated with the

¹ The potential temperature at a pressure level is the temperature that the air would have after it is adiabatically brought to a reference pressure.

156 nearby topography (see Figs. 4a and 1) because of the near neutral lapse rates in the
157 mixed UBL and their absence over the rural areas (see Fig. 4b). The upward motion of
158 this magnitude could affect urban weather conditions such as triggering cumulus clouds
159 near the top of the UBL or the urban-rural boundaries (e.g., Bornstein and Lin 2000).

160 Each layer of the surface-rooted “hot plume” over Baltimore (e.g., $\theta' = 2 \sim 1.5^\circ\text{C}$) is
161 generally deeper and more robust than those upstream, i.e., Columbia (see Fig. 4a).
162 Because of the southwesterly advection of the warm air from the upstream UBL, little
163 additional heat from the surface is needed to maintain the warm column above Baltimore.
164 Instead, most of the local surface heat flux is used to heat the column and increase the
165 depth of the mixed UBL. Entrainment into the potentially warmer air aloft helps further
166 increase the temperature in the mixed UBL (e.g., Zhang and Anthes 1982; Oke 1987)
167 leading to the generation of robust hot plumes over the city of Baltimore.

168 To supplement the above results, we conducted a numerical sensitivity experiment in
169 which the urban areas to the southwest of Baltimore are replaced by a vegetated surface
170 (NUH), as indicated by line CD in Fig. 1, while holding all the other parameters identical
171 to the control simulation (CTL) shown in Figs. 2 and 3. The differenced fields of T_{sfc} and
172 surface winds between the CTL and NUH simulations (see Fig. 3b) show a city-wide
173 reduction in T_{sfc} in experiment NUH, with $1.25 - 1.5^\circ\text{C}$ peak differences or more than
174 25% reduction of the UHI effects. Based on observations of Bloomer et al. (2009), also
175 given in Supplementary Fig. A, the $1.25 - 1.5^\circ\text{C}$ cooling corresponds to a reduction of 3-
176 4 ppb ozone and $\sim 2 \mu\text{g m}^{-3}$ particulate matter in the summer. In addition, the well-mixed
177 UBL in the NUH experiment is about 200 m shallower and the hot plume over Baltimore
178 is weaker than that in CTL (see Figs. 4a and 4b). Vertical motion to the south of

179 Baltimore is mostly downward due to the Bermuda high, confirming further the
180 importance of the urban-surface-rooted hot plumes in generating the pronounced upward
181 motion. Upstream urbanization also appears to cause (see Figs. 3 and 4) enhanced
182 convergence along the Bay and greater intrusion of the Bay breeze into the city of
183 Baltimore.

184 In another sensitivity simulation, Baltimore is treated as a rural area (i.e., the area to
185 the northeast of line CD in Fig. 1) while holding the other conditions identical to the
186 control simulation. Although there is little change in T_{sfc} over Washington, and Columbia
187 (see Supplementary Figs. B1 and B2), Baltimore's T_{sfc} is higher than expected for a
188 "rural" area, offering additional evidence for a non-local UHI effect involving advection
189 of warmer air from upstream.

190 **4. Concluding remarks**

191 In this study, we tested the hypothesis that the UHI effects can be markedly
192 enhanced by upstream urbanization. This is achieved by performing high-resolution
193 control and sensitivity simulations of an extreme UHI event that occurred over Baltimore
194 on 9 July 2007, using a coupled WRF-Noah-UCM model with the finest grid size of 500
195 m. It is found that the coupled model could reproduce the observed UHI effects in terms
196 of T_{skin} and T_{sfc} , such as the 5°C (10°C) T_{sfc} (T_{skin}) contrasts between the urban and rural
197 areas, and the Bay breezes. In particular, the vertical growth of the UHI effects is shown
198 as layered "hot plumes" that are rooted at the urban surfaces with pronounced rising
199 motions.

200 A comparison between the control and sensitivity simulations reveals the important
201 roles of upstream urbanization in enhancing the UHI effects over Baltimore through the

202 (nonlocal) advective processes. Without the upstream influences, the UHI effects over
203 Baltimore would be 1.25°C colder or reduced by 25%, with a 200-m shallower mixed
204 UBL and a much less robust “hot plume”. The enhanced UHI effects are argued to result
205 from the (nonlocal) thermal advection of warm air upstream, the local upward surface
206 heat fluxes and entrainment of the potentially warmer air aloft.

207 Our study shows that while individual cities alone can do little to diminish the
208 harmful impacts of global climate change they can take steps to mitigate changes in local
209 climate. By taking into consideration the interaction of surface properties with
210 atmospheric physics, chemistry and dynamics, informed choices in land use can help
211 lessen heat waves and smog episodes. This could be an especially powerful tool in the
212 developing world where urbanization is proceeding rapidly and adverse impacts on the
213 environment and human health are substantial.

214 **Acknowledgements**

215 We wish to thank Dr. Fei Chen of the National Center for Atmospheric Research for
216 his helpful advice, and two anonymous reviewers for their helpful comments. This work
217 was funded by Maryland’s Department of Environment.

218

219

References

- 220 Banta, R. M., C. J. Senff, A. B. White, M. Trainer, R. T. McNider, R. J. Valente, S. D.
221 Mayor, R. J. Alvarez, R. M. Hardesty, D. Parrish, F. C. Fehsenfeld, (1998), Daytime
222 buildup and nighttime transport of urban ozone in the boundary layer during a
223 stagnation episode, *J. Geophys. Res.*, **103**, 22519-22544.
- 224 Bloomer, B. J., J. W. Stehr, C. A. Piety, R. J. Salawitch, R. R. Dickerson, (2009),
225 Observed relationships of ozone air pollution with temperature and emissions,
226 *Geophys. Res. Lett.*, **36**, L09803, doi:10.1029/2009GL037308.
- 227 Bornstein, R., and Q. L. Lin, (2000), Urban heat islands and summertime convective
228 thunderstorms in Atlanta: three case studies, *Atmos. Environ.* **34**, 507-516.
- 229 Chen, F., and J. Dudhia, (2001), Coupling an advanced land-surface-hydrology model
230 with the Penn State-NCAR MM5 modeling system. Part I: Model implementation and
231 sensitivity, *Mon. Wea. Rev.*, **129**, 569-585.
- 232 Cheng, Y. Y., and D. W. Byun, (2008), Application of high resolution land use and land
233 cover data for atmospheric modeling in the Houston-Galveston metropolitan area, Part
234 I: Meteorological simulation results, *Atmos. Environ.* **42**, 7795-7811.
- 235 Fischer, P. H., B. Brunekreef, E. Lebret, (2004), Air pollution related deaths during the
236 2003 heat wave in the Netherlands, *Atmos. Environ.* **38**, 1083-1085.
- 237 Grell, G. A., and D. Devenyi, (2002), A generalized approach to parameterizing
238 convection combining ensemble and data assimilation techniques, *Geophys. Res. Lett.*,
239 **29**(14), 1693, doi:10.1029/2002GL015311.
- 240 Grossman-Clarke, S., Y. Liu, J. A. Zehender, J.D. Fast, (2008), Simulations of the urban
241 planetary boundary layer in an arid metropolitan area. *J. Appl., Meteor. Climatol.*, **47**,

242 752-768.

243 Hong, S.Y., J. Dudhia, and S. H. Chen, (2004), A revised approach to ice microphysical
244 processes for the bulk parameterization of clouds and precipitation, *Mon. Wea. Rev.*,
245 **132**, 103–120.

246 IPCC, (2007), *Intergovernmental Panel on Climate Change: Fourth Assessment Report*.
247 University Press, Cambridge, 104pp.

248 Janjić, Z. I., (1994), The step-mountain Eta coordinate model: Further development of the
249 convection, viscous sublayer and turbulent closure schemes. *Mon. Wea. Rev.*, **122**,
250 927–945.

251 Jacob, D. J., D. A. Winner, (2009), Effect of climate change on air quality, *Atmos.*
252 *Environ.*, **43**, 51-63.

253 Kalnay, E., and M. Cai, (2003), Impact of urbanization and land-use change on climate,
254 *Nature*, **423**, 528-531, doi: 10.1038/nature01675.

255 Kusaka, H., H. Kondo, Y. Kikegawa, and F. Kimura, (2001), A simple single-layer urban
256 canopy model for atmospheric models: Comparison with multi-layer and slab models,
257 *Bound.-Layer Meteor.*, **101**, 329-358.

258 Oke, T. R., (1973), City size and the Urban Heat Island. *Atmos. Environ.*, **7**, 769-779

259 Oke, T. R., and H. A. Cleugh, (1987), Urban heat-storage derived as energy-balance
260 residuals, *Bound.-Layer Meteor.*, **39**, 233-245.

261 Rotach, M. W. L., R. Vogt, C. Bernhofer, E. Batchvarova, A. Christen, A. Clappier, B.
262 Feddersen, S. E. Gryning, G. Martucci, H. Mayer, V. Mitev, T. R. Oke, E. Parlow, H.
263 Richner, M. Roth, Y. A. Roulet, D. Ruffieux, J. A. Salmond, M. Schatzmann, J. A,
264 Voogt, (2005), BUBBLE - An urban boundary layer meteorology project, *Theor. Appl.*

265 *Climatol.* **81**,231-261.

266 Skamarock, W. C., J. B. Klemp, J. Dudhia, D. O. Gill, D. M. Barker, W. Wang, and J.G.

267 Powers, (2005), *A description of the Advanced Research WRF Version 2*, NCAR,

268 100pp.

269 Stedman, J. R., (2004), The predicted number of air pollution related deaths in the UK

270 during the August 2003 heatwave, *Atmos. Environ.* **38**, 1087-1090.

271 Zhang, D.-L., and R. A. Anthes, (1982), A high-resolution model of the planetary

272 boundary-layer-sensitivity tests and comparisons with SESAME-79 data, *J. Appl.*

273 *Meteor.*, **21**,1594-1609.

274

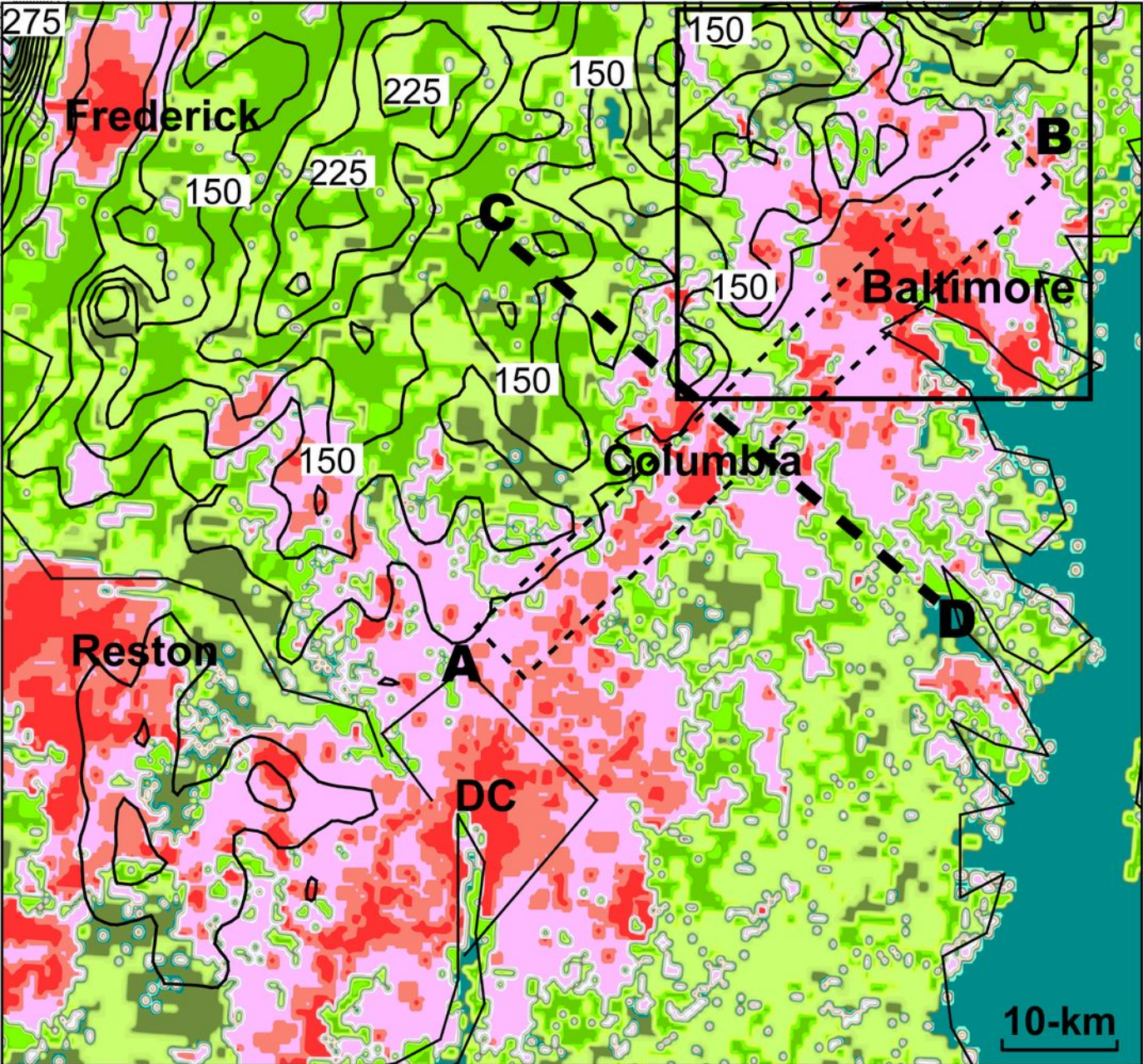
Figure Captions

275
276 **Figure 1.** Dominant land-use (shaded) and elevation (solid lines, at intervals of 25 m
277 starting from 125 m) over a subdomain of the finest-resolution mesh. The zone AB
278 enclosed by dashed lines denotes the location of the area-averaged vertical cross
279 section used in Fig. 4; the squared box is the subdomain used in Fig. 3; and line CD
280 indicates the boundary of land-use changes used in sensitivity experiments.

281 **Figure 2.** Horizontal distribution of skin temperature ($^{\circ}\text{C}$, shadings) at 1745 UTC 9 July
282 2007: (a) observed by the MODIS satellite; and (b) simulated with surface ($z = 10$
283 m) wind vectors (m s^{-1}) superposed. White wind barbs in (b) denote a few observed
284 surface winds; a full barb is 5 m s^{-1} .

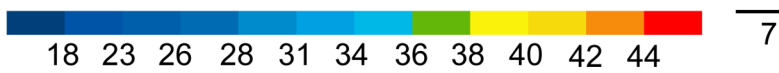
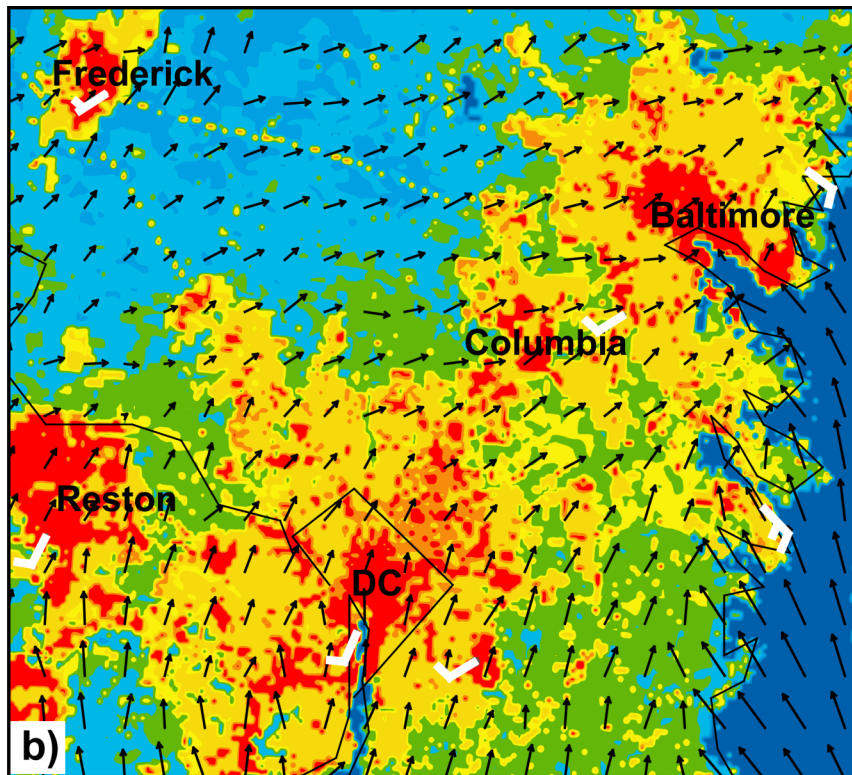
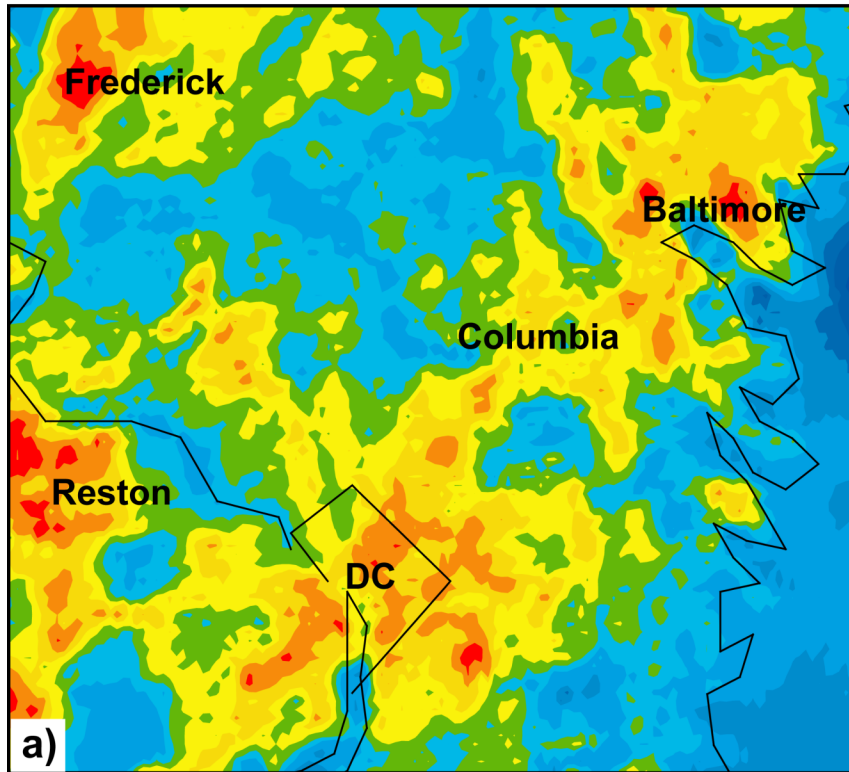
285 **Figure 3.** Horizontal distribution of (a) surface temperature ($^{\circ}\text{C}$, shaded) and wind
286 vectors (m s^{-1}) around Baltimore from the 56.5-h control (CTL) run, valid at 2030
287 UTC 9 July 2007; and (b) as in (a) but for the differenced fields between the CTL
288 and NUH (no urbanization to the south of Baltimore) runs (i.e., CTL – NUH).

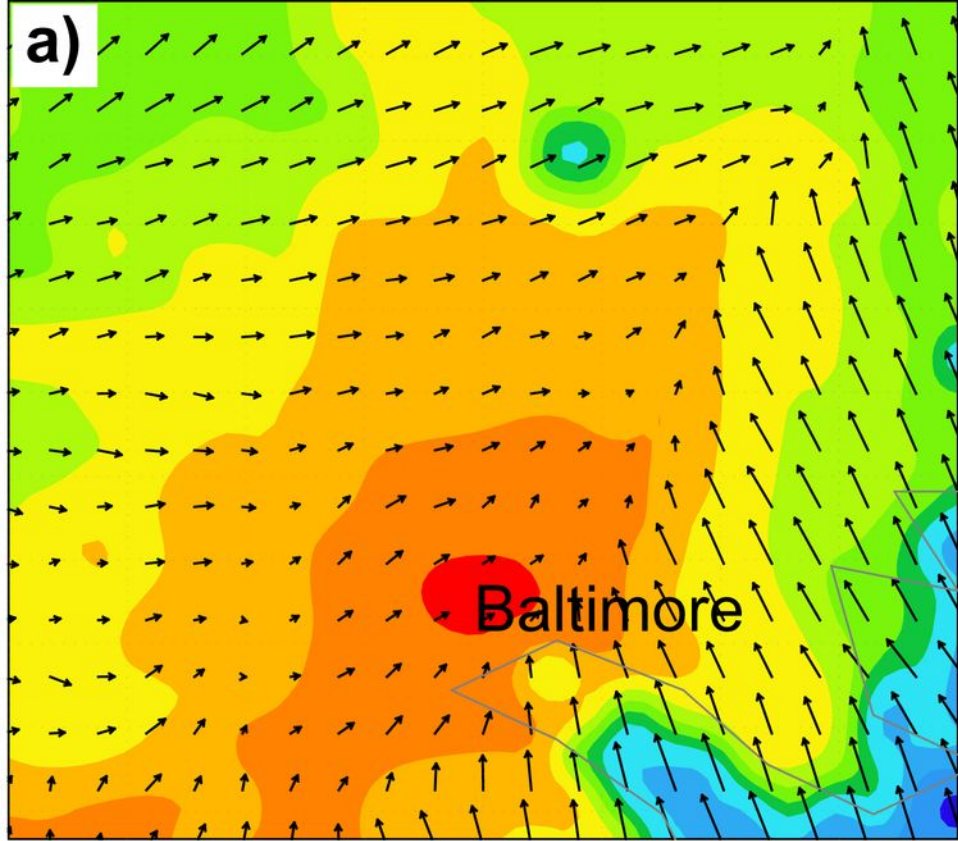
289 **Figure 4.** Comparison of the vertical cross sections of potential temperature perturbations
290 (θ') ($^{\circ}\text{C}$, shaded) and upward motion (gray lines, m s^{-1}), superposed with in-plane
291 flow vectors (m s^{-1}), from the 56.5-h simulations valid at 2030 UTC 9 July 2007,
292 between (a) the control run; and (b) the no urbanization to the south of Baltimore
293 run. They are taken from zone AB (see Fig. 1).



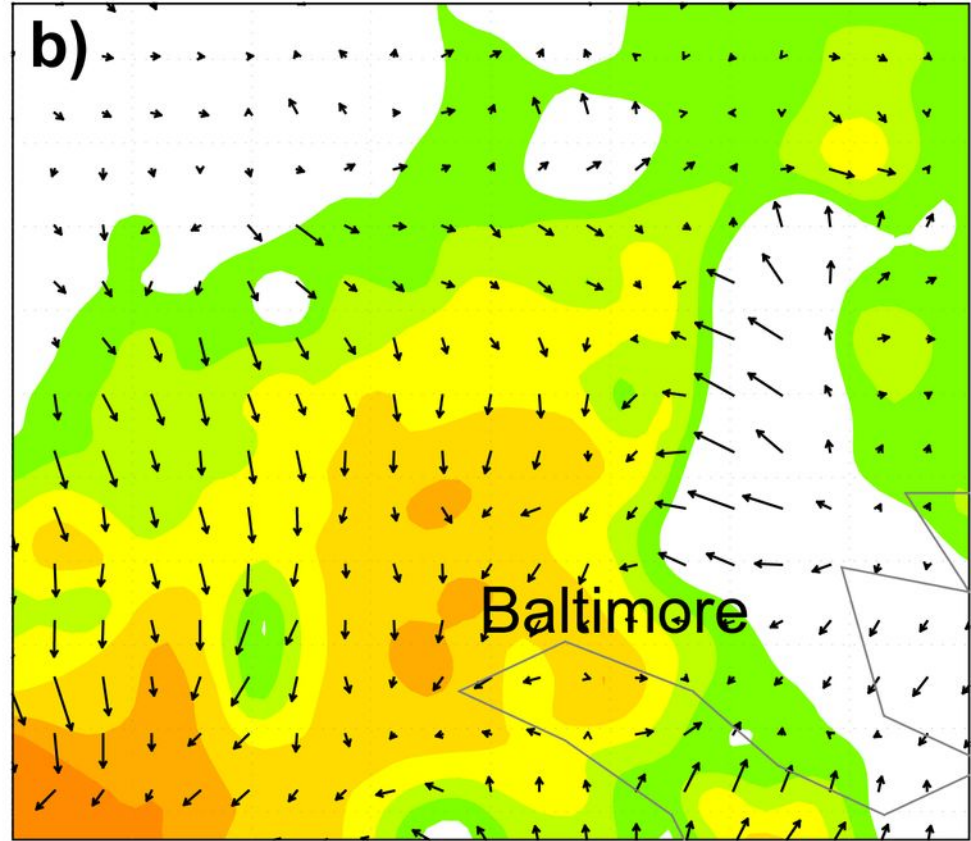
- | | |
|---|--|
| ■ Industr./commer./transp. | ■ Mixed Forest |
| ■ High Inten. Residential | ■ Deciduous Broadleaf Forest |
| ■ Low Inten. Residential | ■ Cropland/Grassland Mosaic |
| ■ Water Bodies | ■ Cropland/Woodland Mosaic |

2007-07-09-1745UTC





27 28 29 30.5 31.5 32.5 33.5 34.5 35.5 36.5



0 0.25 0.5 0.75 1 1.25

